Charge-Discharge Characteristics of Li/CuCl_2 Batteries with LiPF_6/Methyl Difluoroacetate Electrolyte

Hashizaki, Katsuo
Institute for Materials Chemistry and Engineering, Kyushu University

Dobashi, Shinsaku
Office of Society-Academia Collaboration for Innovation, Kyoto University

Okada, Shigeto
Institute for Materials Chemistry and Engineering, Kyushu University

Hirai, Toshiro
Office of Society-Academia Collaboration for Innovation, Kyoto University

他

https://doi.org/10.5109/2320995

出版情報：Evergreen. 6 (1), pp.1-8, 2019-03. 九州大学グリーンアジア国際リーダー教育センター
バージョン：
権利関係：

Charge-Discharge Characteristics of Li/$CuCl_2$ Batteries with $LiPF_6$/Methyl Difluoroacetate Electrolyte

Katsuo Hashizaki[1,*], Shinsaku Dobashi[2,3], Shigeto Okada[1], Toshiro Hirai[2], Jun-ichi Yamaki[2], Zempachi Ogumi[2]

[1]Institute for Materials Chemistry and Engineering, Kyushu University, Japan

[2]Office of Society-Academia Collaboration for Innovation, Kyoto University, Japan

[3]Research & Innovation Center, Mitsubishi Heavy Industries, Ltd., Japan

*Author to whom correspondence should be addressed,

E-mail: 3ES16003G@s.kyushu-u.ac.jp

(Received December 21, 2018; accepted January 17, 2019).

As conversion-type cathode materials, transition-metal chlorides are known to suffer from dissolution in organic solvents. However, our previous investigation revealed that in the Li/$CuCl_2$ battery, the dissolution of $CuCl_2$/C cathode materials could be suppressed by using $LiPF_6$/methyl difluoroacetate (MFA; CHF_2COOCH_3) electrolyte. Consequently, its capacity decline was lessened by raising the charged voltage. Herein we examine the re-conversion reaction cathode of Cu/LiCl instead of the conversion reaction cathode of $CuCl_2$/C. The charge-discharge characteristics of both electrodes are reported. The Cu/LiCl electrode with $LiPF_6$/MFA could charge and discharge without carbon additives.

Keywords: $CuCl_2$, LiCl, Cu, conversion, re-conversion, Lithium ion battery, MFA, $LiPF_6$

1. Introduction

Lithium-ion batteries (LIBs) are widely used as electrical energy storage components for portable electronic devices, electric vehicles (EVs), electrical energy storage system (EES or ESS), and electric power control system of photovoltaic and/or wind-turbine power generation. In particular, the portable devices and EVs require light weight, compact LIBs with good long-term performance.

While the demand for LIBs with higher energy density continues[1)-3)], the electrical energy density of conventional LIBs is already approaching the theoretical limit of the electrode materials, whose Li storage capacity is limited by the number of available sites in the host lattice, and by the redox competition with other phases. Therefore, it is indispensable to develop high energy density LIBs based on new concepts. Among the many studies on improving the cathode, anode, and electrolyte materials in LIBs[4)-10)], cathodes based on conversion reaction can offer greatly increased capacity compared to intercalation-based cathodes. These cathode materials are completely changed in their structure and chemical identity during charge-discharge. If this feature can be used adequately, such cathodes may yield extremely high capacity via the following general electrochemical conversion reaction between the cathode material and Li-ions[7)]:

$$M_aX_b + nbLi^+ + nbe^- \rightleftarrows bLi_nX + aM \quad [1]$$

where M is a transition metal (Cu, Fe, Co, Ni, Bi, etc.), X is an anion (O, F, S, N, P, etc.), b is the formal oxidation state of X, and n = 1–3.

Until now, very few studies have considered transition-metal chlorides for conversion-based LIBs. The reason is that they are soluble in many non-aqueous electrolytes[11),12)], leading to increased self-discharge. However, our recent investigations showed that the $LiPF_6$/methyl difluoroacetate (MFA) electrolyte is effective for suppressing self-discharge in Li/$CuCl_2$ batteries[13)]. Li/$CuCl_2$ batteries are promising in terms of their high voltage (3.07 V vs. Li^+/Li) and high capacity (399 mAh g^{-1}) due to the 2-electron redox reaction $CuCl_2 + 2Li^+ + 2e^- \rightleftarrows Cu + 2LiCl$. They also have the characteristics of lower overvoltage during discharge and charge, compared to any Li/transition-metal fluorides[14)-25)], sulfides[26)-40)], and oxides[41)-54)] used in conversion-based LIBs. Additionally, the majority of published studies in this area focus on discharge starting from the M_aX_b electrode, while those about charge starting from the M/Li_nX electrode are few[55),56)]. In the $CuCl_2$ electrode based on conversion reaction, the Li^+ ions need to be supplied by the lithium metal anode. In contrast, Li^+ is already included in the Cu/LiCl electrode based on re-conversion reaction. Hence, the latter could allow the use of graphite instead of lithium metal anode, thereby improving the battery safety. Moreover, since the conventional intercalation-type lithium ion batteries also

use graphite anodes, their energy density can be dramatically increased by merely switching the cathode to the Cu/LiCl electrode. Thirdly, the Cu/LiCl electrode initially contains the highly conductive copper, therefore it has a lower need of carbon for conductivity, further increasing the energy density. Additionally, $LiPF_6$/MFA is known to improve the thermal stability of LIBs [57)-63)]. Thus, the combination of re-conversion-based LIBs with Cu/LiCl cathode and the $LiPF_6$/MFA electrolyte could improve not only the electrical energy density, but also the safety of LIBs.

Based on previous characterization of the $CuCl_2$/C electrode with $LiPF_6$/MFA[13)], in this work we first evaluate the effect of raising the charged upper limit voltage from 3.6 to 4.0 V. Then the Cu/LiCl electrode was investigated as a re-conversion reaction cathode with $LiPF_6$/MFA in LIBs. The mechanisms of the re-conversion reaction, and the fundamental characteristics of the charge and discharge processes were examined. The reaction mechanisms of $CuCl_2$/C and Cu/LiCl electrodes were also discussed.

2. Experimental

Cu/LiCl electrodes and $LiPF_6$/MFA electrolytes were prepared under inert gas and dry conditions (O_2 concentration: < 1 ppm; dew point: < −80 °C) inside an Ar-filled glove box (Miwa Mfg. Co. Ltd.). The cathode Cu/LiCl electrodes were prepared by mixing Cu powder (Kojundo Chemical Laboratory Co. Ltd, CUE08PB), anhydrous LiCl (Sigma-Aldrich Co. LLC, 429457-25G), and polytetrafluoroethylene (PTFE; Du Pont-Mitsui Fluorochemicals Co. Ltd., 6J) in two different weight ratios (Cu:LiCl:PTFE = 40:50:10 and 25:65:10). Prior to mixing, LiCl was crushed in a mortar into particles tens of microns in size. The cathode materials were mixed in the mortar, and rolled into 150 μm-thick sheets. Discs 5 mm in diameter were punched out of the composite sheets, and then pressed onto a Pt mesh (Sanwakinzoku Co., 100 mesh) at 10 MPa pressure to prepare the Cu/LiCl electrodes. The $CuCl_2$/C electrodes were prepared as described in a previous paper[13)]. The carbon material used was acetylene black (AB, DENKA BLACK). The composition was $CuCl_2$:AB:PTFE = 70:25:5 in weight. Pure lithium foil (thickness: 200 μm, Honjo Metal Co. Ltd.) was used as the counter electrode.

MFA (Tokyo Chemical Industry Co. Ltd.) was used as the electrolyte solvent, and its water content was ≤ 50 ppm and the purity was > 99%. The salt $LiPF_6$ was dissolved in MFA at 2.2 mol L^{-1}, a concentration found to produce the lowest self-discharge in our previous study[13)].

A three-electrode electrochemical cell (EC Frontier Co. Ltd.) was used for the charge and discharge measurements. The cathode, counter electrode, and Li metal wire (φ = 1 mm, Honjo Metal Co. Ltd.) reference electrode were assembled in an Ar-filled glove box. Measurements of the electrochemical cell were performed sequentially in the glove box at room temperature with a potentio/galvanostat (Bio-Logic Science Instruments SAS, VSP-300, SP-200). The charged upper limit voltage and discharged lower limit voltage were 4.0 and 2.5 V, respectively, and the charge and discharge current rates were both 0.01 C. Here, C means a current value for completely charging (or discharging) the theoretical capacity of the battery in 1 hour.

The microstructure of the Cu/LiCl electrode surface was observed by scanning electron microscopy (SEM, HITACI FE-SEM SU6600), and the element mapping was conducted by energy dispersive X-ray spectroscopy (EDX, HORIBA EMAX ENERGY EX-X50). The structure of the Cu/LiCl electrode was also characterized by X-ray diffraction (XRD, Bruker Co. D8 ADVANCE). Prior to the SEM-EDX and XRD measurements, the electrochemical cell was disassembled. The Cu/LiCl electrode was rinsed with MFA and dried in Ar-filled glove box before placement in the vessel and/or sample holder.

3. Results and Discussion

3.1 Discharge-charge electrochemical profiles of $CuCl_2$/C electrode

The fundamental electrochemical reactions of Li/$CuCl_2$ batteries are the following redox reaction equations [2] and [3], which sum up to reaction [4]:

$CuCl_2 + Li^+ + e^- \rightleftarrows CuCl + LiCl$ (3.41 V vs. Li^+/Li) [2]

$CuCl + Li^+ + e^- \rightleftarrows Cu + LiCl$ (2.74 V vs. Li^+/Li) [3]

$CuCl_2 + 2Li^+ + 2e^- \rightleftarrows Cu + 2LiCl$ (3.07 V vs. Li^+/Li) [4]

Our previous study reported the cycling performance of the Li/$CuCl_2$ batteries with 2.2 mol L^{-1} $LiPF_6$/MFA. The charge-discharge conditions were: charged upper limit voltage: 3.6 V, discharged lower limit voltage: 2.5 V, and discharge and charge currents: 0.01 C[13)]. In the first discharge process, the first clear plateau at 3.4 V was attributed to the Cu reduction reaction [2], and the second clear plateau at 2.7 V to the Cu reduction reaction [3]. These reactions indicate that the typical electrochemical reaction of Li/$CuCl_2$ batteries is the 2-electron redox reaction of $CuCl_2$ according to equation [4]. Both reactions [2] and [3] were reflected clearly in the discharge profiles. Most remarkably, there was scarcely any overvoltage. Such effective control of the dissolution of cathode materials would allow the discharge and charge of the $CuCl_2$/C electrode as a conversion reaction cathode.

However, during the first charge, the charged capacity was about 230 mAh g^{-1}, which was merely about half of the theoretical capacity of the Li/$CuCl_2$ battery (399 mAh g^{-1}). The second discharge capacity was similarly reduced. In the second cycle, the capacity declined significantly especially at the 3.4 V plateau, due to the disproportionation reactions with co-existing Cu^{2+}, Cu^+, and Cu^0. Consequently, $CuCl_2$ was not formed or deposited on the electrode in the first cycle, according to the X-ray absorption fine structure (XAFS) analysis results. Only CuCl and Cu were detected in the cathode electrode under

the fully charged condition[64]. Based on these results, the charged upper limit voltage was raised from 3.6 to 4.0 V in the current study to promote the formation and deposition of $CuCl_2$.

Fig. 1 shows the cycling performance of the Li/$CuCl_2$ battery with $LiPF_6$/MFA and the charged upper limit voltage of 4.0 V. After the first charge following the first discharge, the charged capacity (based on the weight of $CuCl_2$) rose from 230 to about 280 mAh g^{-1}. Raising the charged voltage clearly changed the appearance of the plateau at 3.4 V during discharge that is attributed to reaction [2], thereby substantially reducing the capacity decline during the second discharge. A few shoulder peaks were observed between 3.6–4.0 V under the higher charge voltage. They may correspond to electrochemical reactions that promoted the formation of $CuCl_2$.

Fig. 2 shows the effect of raising the charged voltage on the cycling discharge capacity. The discharge capacity above 200 mAh g^{-1} is thought to correspond to the electrochemical reaction [2]. The 2nd and 3rd discharge capacities were higher when the charged voltage was changed from 3.6 to 4.0 V.

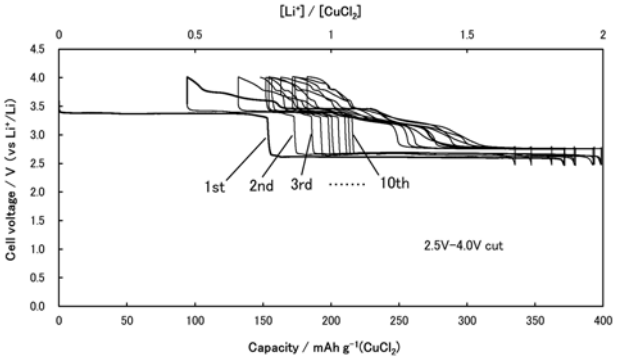

Fig. 1: Discharge and charge profiles of the $CuCl_2$/C electrode in 2.2 mol L^{-1} $LiPF_6$/MFA, with the charged upper limit voltage of 4.0 V at 0.01C (0.071mA/cm^2).

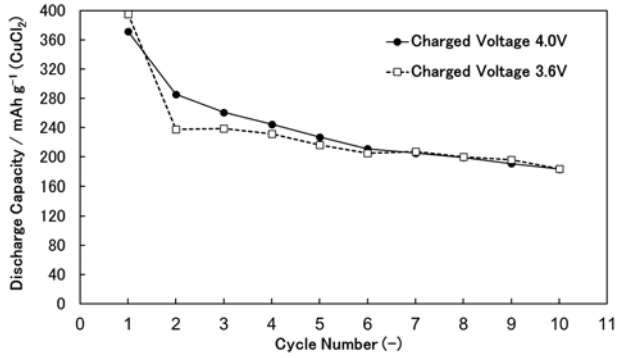

.**Fig. 2:** Influence of cycling on the discharge capacity with different charged upper limit voltages in 2.2 mol L^{-1} $LiPF_6$/MFA.

Therefore, the additional electrochemical reactions that promoted the formation/deposition of $CuCl_2$ due to raised charged voltage also reversed the decay of the discharged capacity.

3.2 Charge-discharge electrochemical profiles of Cu/LiCl electrode

The above discussion focused on the discharge-charge characteristics of the discharge-starting $CuCl_2$/C electrode as a conversion reaction cathode. Now we examine the fundamental charge-discharge characteristics of the charge-starting Cu/LiCl electrode as a re-conversion reaction cathode. The Cu/LiCl electrode originally contained copper, which could function in place of carbon as a highly conductive material. Therefore, first we investigate the characteristics of the Cu/LiCl electrode without added carbon.

Prior to the charge and discharge measurements, cyclic voltammetry (CV) scans were recorded at a rate of 0.01 mV s^{-1} to confirm the oxidation and reduction potentials of the Cu/LiCl electrode (Cu:LiCl:PTFE = 40:50:10) with $LiPF_6$/MFA. As shown in **Fig. 3**, the CV profiles are very simple and clearly reflect the electrochemical characteristics of Li/$CuCl_2$ batteries.

In the first cycle, the Cu oxidation and reduction were largely unobservable. However, two oxidation peaks and one reduction peak were clearly observed after the second cycle. This indicates that the Cu/LiCl electrode had poor conductivity during the first charge-discharge cycle, possibly due to the large particle size (1 μm) in the initial copper powder. After the second cycle, a higher electric current flow was observed, because the dispersed copper nanoparticles formed by the first re-conversion reaction increased the conductivity of the electrode.

On the oxidation side, the first sharp oxidation peak of the Cu/LiCl electrode is attributed to reaction [3], and the second broad oxidation at around 3.6 V is attributed to

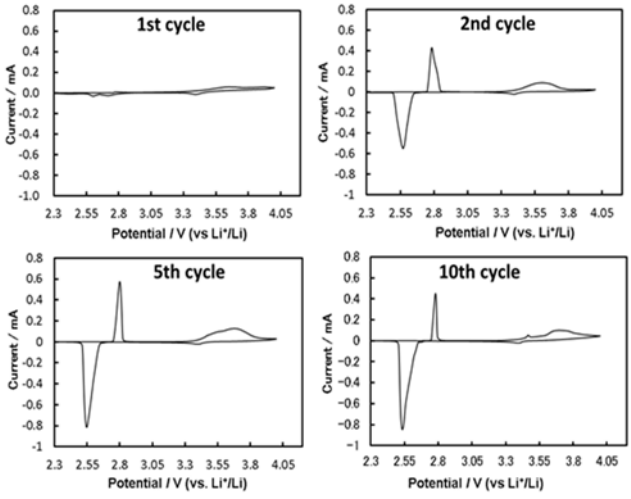

Fig. 3: CV profiles (cycles 1, 2, 5, and 10) of the Cu/LiCl electrode (Cu:LiCl:PTFE = 40:50:10) with 2.2 mol L^{-1} $LiPF_6$/MFA. The scan rate was 0.01 mV s^{-1}.

reaction [2]. As discussed earlier, disproportionation reactions (i.e., Cu^{2+}+ Cl^-+e^- ⇄ CuCl and Cu^+ + e^- ⇄ Cu) could occur with the coexistence of Cu^{2+}, Cu^+, and Cu^0, and CuCl is close to an electrical insulator, thereby making

the synthesis of $CuCl_2$ difficult during the charge process, and limiting the charge just over ~200 mAh g^{-1}.

On the reduction side, only one distinguishable sharp reduction peak was observed and attributed to reaction [3]. It is believed that the formation of $CuCl_2$ is obstructed by the disproportionation reactions, and only CuCl was formed/reduced during the charge/discharge processes according to X-ray absorption fine structure analysis. This is also suggested by the fact that the charge and discharge capacities were only about 200 mAh g^{-1}.

Fig. 4 shows the charge and discharge profiles of the Cu/LiCl electrode (Cu:LiCl:PTFE = 40:50:10) with $LiPF_6$/MFA. From the results of **Fig. 3**, the charged upper limit and discharged lower limit voltages were 4.0 and 2.5 V, respectively. The capacity is based on the total weight of Cu and 2LiCl, which is the stoichiometric ratio to synthesize $CuCl_2$ in the cathode electrode. As mentioned earlier, the initial Cu and LiCl mixture had poor conductivity as the coarse copper particles did not form a sufficient electron path. Therefore, the charged voltage was high in the first Cu oxidation process and the charged capacity was low, making the total profiles shift to the negative side.

The capacity increased gradually during repeated charge and discharge as fine copper particles precipitated. However, after five cycles, this capacity decreased slowly. This is attributed to the slight dissolution of Cu and/or LiCl in the electrolyte, as well as changes in the cathode material structure accompanying the anion (Cl^-) exchange peculiar to the re-conversion reaction. The most characteristic feature observed in **Fig. 4** is that, while the first clear plateau was attributed to the Cu oxidation reaction [3], the second plateau at ~3.4 V had a mild slope without clear plateau (similar to the first plateau at 2.7 V) that would be attributed to reaction [2].

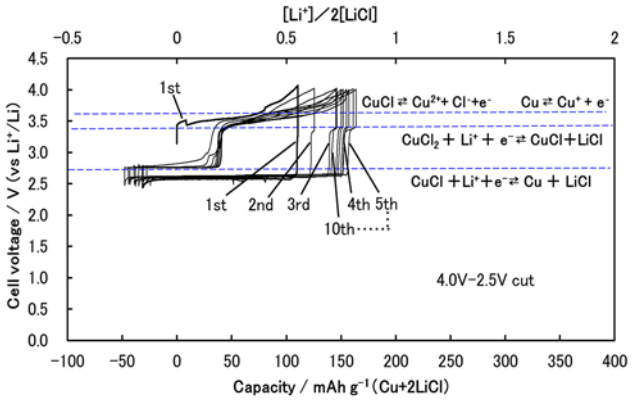

Fig. 4: Charge and discharge profiles of the Cu/LiCl electrode (Cu:LiCl:PTFE = 40:50:10) with 2.2 mol L^{-1} $LiPF_6$/MFA at 0.01C (0.19mA/cm^2). The capacity is based on the total weight of Cu and 2LiCl.

The electrochemical reactions, such as $CuCl \rightleftarrows Cu^{2+} + Cl^- + e^-$ (3.6 V vs. Li^+/Li), and/or $Cu \rightleftarrows Cu^+ + e^-$ (3.6 V vs. Li^+/Li) would occur at the same time in the charge process. In the discharge process, an initial plateau at ~3.4 V corresponding to [2] was visible, but the plateau was not extended. Only the plateau due to reaction [3] was clearly observed.

These behaviors are attributed to the copper disproportionation reactions. Accordingly, the utilization of copper stayed at nearly 50%, which is the same as that for the $CuCl_2$/C electrode in the charge process. The charge-discharge profiles of the Cu/LiCl electrode are very simple compared with those of the $CuCl_2$/C electrode, especially the absence of the shoulder at 3.2 V. It is thought that carbon in the electrode caused side reactions and affected the charge and discharge.

Fig. 5 and **Fig. 6** show the SEM images and EDX elemental mapping results of Cu, Cl, and F in the Cu/LiCl electrode (Cu:LiCl:PTFE = 40:50:10), both in pristine condition and after 10 cycles of charge-discharge measurements at the constant current rate of 0.01 C (0.19mA/cm^2). During cycling, highly dispersed copper and LiCl nanoparticles precipitated visibly in the cathode electrode. After 10 cycles, connected cluster particles of Cu and LiCl about 5 μm in size were formed. These finely dispersed, connected clusters maintained good conductivity in place of added carbon.

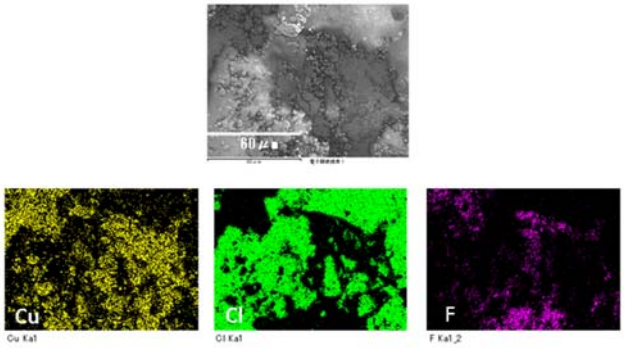

Fig. 5: SEM image (top) and EDX elemental color maps of Cu, Cl, and F (bottom) in the original Cu/LiCl electrode (Cu:LiCl:PTFE = 40:50:10).

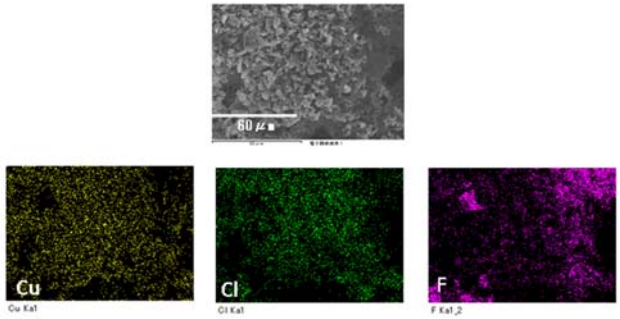

Fig. 6: SEM image (top) and EDX elemental color maps of Cu, Cl, and F (bottom) in the Cu/LiCl electrode (Cu:LiCl:PTFE = 40:50:10) after 10 cycles of charge and discharge measurements.

In **Fig. 6**, the Cu and Cl elements dispersed finely and uniformly over the entire electrode. A small amount of F was observed, and attributed to the PTFE and LiF derived from the decomposition of $LiPF_6$. The dispersion of F

seems to be affected by repeated charge-discharge re-conversion reactions. The self-precipitation process, and the control of disproportionation reactions of copper would permit the Cu/LiCl electrode to function as a charge-starting cathode in re-conversion-based LIBs without added carbon for conductivity. Nevertheless, since the structure of the cathode based on re-conversion reaction changes during each charge and discharge process, the cathode performance depends greatly on the experimental conditions, such as the mixing of electrode materials, the current rate, and the temperature.

Fig. 7 shows the charge and discharge profiles of the Cu/LiCl electrode with excess LiCl (Cu:LiCl:PTFE = 25:65:10) with $LiPF_6$/MFA, using the same charged upper limit and discharged lower limit voltages as the electrode with Cu:LiCl:PTFE = 40:50:10. The content ratio of LiCl was raised to twice the stoichiometric value for synthesizing $CuCl_2$, in order to examine how the excess chlorine element addition in cathode affects the charge-discharge profiles (especially the moderate second plateau in the charge process) and the precipitation of $CuCl_2$. The precipitation of $CuCl_2$ would be expected depending on the excess addition of chlorine in cathode. The capacity in **Fig. 7** is based on the total weight of Cu and 4LiCl within the electrode.

The results show that increasing the amount of LiCl stabilized the charge and discharge profiles, and restrained the capacity decline. However, the initial plateau at 3.4 V that corresponds to the Cu reduction reaction [2] was not as extended as in the electrode with Cu:LiCl:PTFE = 40:50:10. The utilization of copper stayed at nearly 50%, the same as in the $CuCl_2$/C electrode. Therefore, increasing the amount of LiCl only affected the stability of electrochemical reactions in the electrode and electrolyte.

Fig. 8 shows the SEM images and EDX elemental color maps of Cu, Cl, and F in the Cu/LiCl electrode with excess LiCl after 9.5 cycles (i.e., fully charged). When the figure is compared with that for the electrode with Cu:LiCl:PTFE = 40:50:10 (**Fig. 6**), the content of F element (which seems to be LiF derived from the decomposition of $LiPF_6$) was remarkably increased, despite the different charged conditions. The electrode surface was covered by hard crystallized materials, which are thought to be LiF (derived from the decomposition of $LiPF_6$) or LiCl. The former is deposited on the electrode due to its poor solubility. The latter is only slightly soluble in the electrolyte, therefore it re-precipitates significantly during discharge on the electrode surface. These deposits may protect the Cu/LiCl electrode surface, by hindering the dissolution of Cu and $CuCl_2$ in the electrolyte, and constraining the structural change of the electrode during the re-conversion reaction.

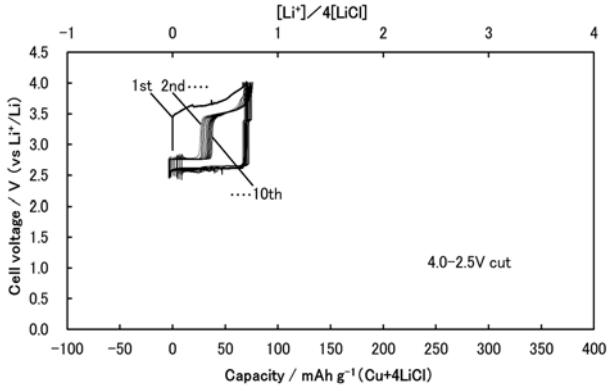

Fig. 7: Charge and discharge profiles of the Cu/LiCl electrode (Cu:LiCl:PTFE = 25:65:10) with 2.2 mol L^{-1} $LiPF_6$/MFA at 0.01C (0.11mA/cm^2).

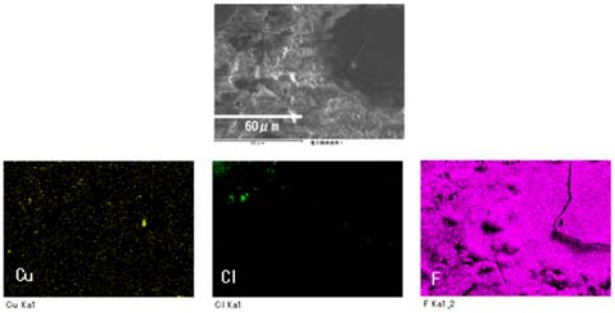

Fig. 8: SEM image (top) and EDX elemental color maps of Cu, Cl, F, and P (bottom) in the Cu/LiCl electrode (Cu:LiCl:PTFE = 25:65:10) after 9.5 cycles of charge and discharge measurements.

Fig. 9 compares the cycling performance between these two Cu/LiCl electrodes. The discharged capacities are based on the weight of stoichiometrically synthesized $CuCl_2$ (which is limited by the amount of copper) in each electrode. The electrode with excess LiCl had a higher initial discharged capacity which also declined slower. The difference is attributed to the excess LiCl, as well as other small variations such as the battery capacity (3.78 mAh for the electrode with Cu:LiCl:PTFE = 40:50:10 and 2.22 mAh for the one with Cu:LiCl:PTFE = 25:65:10). Additionally, when the LiCl content is higher, the coverage of the electrode surface by precipitated LiCl and LiF could suppress the dissolution of active cathode materials.

Finally, we investigate whether the Cu/LiCl electrode with excess LiCl in the fully charged condition (after 9.5 cycles) can form $CuCl_2$. **Fig. 10** shows the corresponding XRD patterns, plus typical patterns of $CuCl_2$ and CuCl for reference. Under the fully charged condition, only CuCl and LiCl signals were detected, but not $CuCl_2$. The absence of $CuCl_2$ signal could be attributed to the instability of Cu^{2+} due to disproportionation reactions in the electrolyte at moderate oxidation potential (around 3.6V). The corresponding electrochemical reaction potential could be influenced by the existence of chloride ions in the solvent.

As both Cu/LiCl electrodes only reached just half of the theoretical capacity of 399 mAh g^{-1}, the disproportionation reactions should also occur in both of them. To improve the performance and Cu utilization efficiency of the Cu/LiCl electrode and promote $CuCl_2$ formation, it would be necessary to add carbon, and to control the ion concentrations in the Cu/LiCl electrode. Especially, the Cl^- ion in the electrochemical reaction field in the electrode has great influence on the copper oxidation-reduction reactions. Our next study will focus on controlling the Cl^- concentration (activity) with added carbon materials.

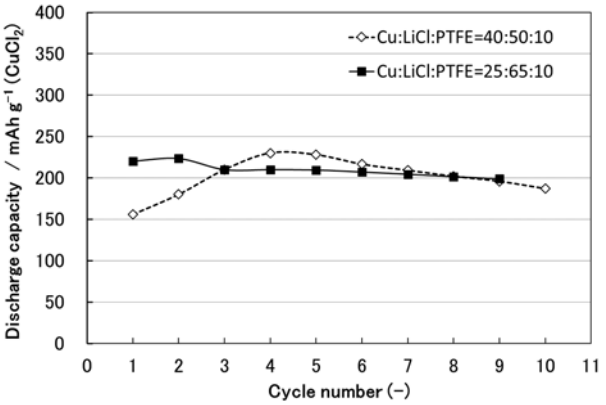

Fig. 9: Comparison of cycling performance between Cu/LiCl electrodes with Cu:LiCl:PTFE = 40:50:10 and 25:65:10.

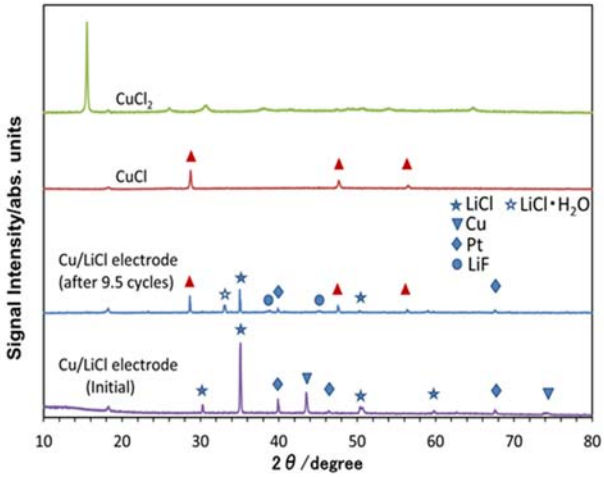

Fig. 10: XRD patterns of Cu/LiCl electrode (Cu:LiCl:PTFE = 25:65:10) after 9.5 cycles. The typical XRD patterns of $CuCl_2$ and CuCl are also shown.

4. Conclusion

We investigated the capacity and characteristics of $CuCl_2$/C and Cu/LiCl electrodes (as conversion and re-conversion cathodes, respectively) with higher charged voltage. The following results were obtained.

1) The $CuCl_2$/C electrode undergoes additional electrochemical reactions that promote the formation of $CuCl_2$ between 3.6–4.0 V.
2) The Cu/LiCl electrode could charge-discharge without carbon additives. Cu oxidation and reduction are believed to occur due to the conductive Cu, which precipitated in the electrode to form dispersed electron path during the reaction with LiCl.
3) In the Cu/LiCl electrode, excess LiCl content can effectively stabilize the charge-discharge performance, due to its role in the condensation of fluorine-containing compounds on the electrode surface.
4) A plateau at 3.4 V during discharge was observed in both electrodes. To promote the formation of $CuCl_2$ during charging, carbon additives may be necessary to control the ion concentrations in the electrochemical reaction field.

Acknowledgements

This work was supported by the RISING Project of the New Energy and Industrial Technology Development Organization (NEDO), Japan.

References

1) B. Dunn, H. Kamath and J. M. Tarascon, *Science*, **334**, 928 (2011).
2) V. Etacheri, R. Marom, R. Elazari, G. Salitra and D. Aurbach, *Energy Environ. Sci.*, **4**, 3243 (2011).
3) J. M. Tarascon and M. Armand, *Nature*, **414**, 359 (2001).
4) S. Goriparti, E. Miele, F. De Angelis, E. Di Fabrizio, R. P. Zaccaria, and C. Capiglia, *J. Power Sources*, **257**, 421 (2014).
5) Y. N. Zhou, M. Z. Xue, and Z. W. Fu, *J. Power Sources*, **234**, 310 (2013).
6) B. Scrosati, and J. Garche, *J. Power Sources*, **195**, 2419 (2010).
7) J. Cabana, L. Monconduit, D. Larcher, and M. R. Palacín, *Adv. Mater.*, **22**, E170 (2010).
8) M. R. Palacín, *Chem. Soc. Rev.*, **38**, 2565 (2009).
9) R. Malini, U. Uma, T. Sheela, M. Ganesan, and N. G. Renganathan, *Ionics.*, **15**, 301 (2009).
10) P. G. Bruce, B. Scrosati, and J. M. Tarascon, Angew. *Chem. Int. Ed.*, **47**, 2930 (2008).
11) J. L. Liu, W. J. Cui, C. X. Wang, and Y. Y Xia, *Electrochem. Commun.*, **13**, 269 (2011).
12) T. Li, Z. X. Chen, Y. L. Cao, X. P. Ai, and H. X. Yang, *Electrochim. Acta*, **68**, 202 (2012).
13) S. Dobashi, K. Hashizaki, H. Yakuma, T. Hirai, J. Yamaki, and Z. Ogumi, *J. Electrochem. Soc.*, **162 (14)**, A2747 (2015).

14) H. Arai, S. Okada, Y. Sakurai, and J. Yamaki, *J. Power Sources*, **68**, 716 (1997).
15) F. Badway, N. Pereira, F. Cosandey, and G. G. Amatucci, *J. Electrochem. Soc.*, **150 (9)**, A1209 (2003).
16) F. Badway, F. Cosandey, N. Pereira, and G. G. Amatucci, *J. Electrochem. Soc.*, **150 (10)**, A1318 (2003).
17) H. Li, P. Balaya, and J. Maier, *J. Electrochem. Soc.*, **151 (11)**, A1878 (2004).
18) Z. W. Fu, C. L. Li, W.Y. Liu, J. Ma, Y. Wang, and Q. Z. Qin, *J. Electrochem. Soc.*, **152 (2)**, E50 (2005).
19) I. Plitz, F. Badway, J. Al-Sharab, A. DuPasquier, F. Cosandey, and G. G. Amatucci, *J. Electrochem. Soc.*, **152 (2)**, A307 (2005).
20) Y. Makimura, A. Rougier, L. Laffont, M. Womes, J. C. Jumas, J. B. Leriche, and J. M. Tarascon, *Electrochem. Commun.*, **8**, 1769 (2006).
21) F. Badway, A. N. Mansour, N. Pereira, J. F. Al-Sharab, F. Cosandey, I. Plitz, and G. G. Amatucci, *Chem. Mater.*, **19**, 4129 (2007).
22) H. Zhang, Y. N. Zhou, Q. Sun, and Z. W. Fu, *Solid State Sci.*, **10**, 1166 (2008).
23) T. Li, L. Li, Y. L. Cao, X. P. Ai, and H. X. Yang, J. *Phys. Chem. C*, **114**, 3190 (2010).
24) C. Li, L. Gu, S. Tsukimoto, P. A. van Aken, and J. Maier, *Adv. Mater.*, **22**, 3650 (2010).
25) N. Yamakawa, M. Jiang, and C. P. Grey, *Chem. Mater.*, **21**, 3162 (2009).
26) F. Bonino, M. Lazzari, B. Rivolta, and B. Scrosati, *J. Electrochem. Soc.*, **131 (7)**, 1498 (1984).
27) J. S. Chung and H. J. Sohn, *J. Power Sources*, **108**, 226 (2002).
28) S. C. Han, H. S. Kim, M. S. Song, J. H. Kim, H. J. Ahn, J. Y. Lee, and J. Y. Lee, *J. Alloys Compd.*, **351**, 273 (2003).
29) A. Hayashi, T. Ohtomo, F. Mizuno, K. Tadanaga, and M. Tatsumisago, *Electrochim. Acta*, **50**, 893 (2004).
30) J. M. Yan, H. Z. Huanga, J. Zhanga, Z. J. Liub, and Y. Yang, *J. Power Sources*, **146**, 264 (2005).
31) A. Debart, L. Dupont, R. Patrice, and J. M. Tarascon, *Solid State Sci.*, **8**, 640 (2006).
32) X. J. Zhu, Z. Wen, Z. H. Gu, and S. H. Huang, *J. Electrochem. Soc.*, **153 (3)**, A504 (2006).
33) Q. Wang, R. Gao, and J. H. Li, *Appl. Phys. Lett.*, **90 (14)**, 143107 (2007).
34) T. Matsumura, K. Nakano, R. Kanno, A. Hirano, N. Imanishi, and Y. Takeda, *J. Power Sources*, **174**, 632 (2007).
35) Q. Wang and J. H. Li, *J. Phys. Chem. C*, **111**, 1675 (2007).
36) J. Z. Wang, S. L. Chou, S. Y. Chew, J. Z. Sun, M. Forsyth, D. R. MacFarlane, and H. K. Liu, *Solid State Ionics*, **179** , 2379 (2008).
37) J. L. Gomez-Camer, F. Martin, J. Morales, and L. Sanchez, *J. Electrochem. Soc.*, **155 (3)**, A189 (2008)
38) T. Takeuchi, H. Sakaebe, H. Kageyama, T. Sakai, and K. Tatsumi, *J. Electrochem. Soc.*, **155 (9)**, A679 (2008).
39) H. Li, W. J. Li, L. Ma, W. X. Chen, and J. M. Wang, *J. Alloys Compd.*, **471**, 442 (2009).
40) R. D. Apostolova, E. M. Shembel, I. Talyosef, J. Grinblat, B. Markovsky, and D. Aurbach, *Russ. J. Electrochem.*, **45 (3)**, 311 (2009).
41) P. Poizot, S. Laruelle, S. Grugeon, L. Dupont, and J. M. Tarascon, *Nature*, **407 (28)**, 496 (2000).
42) S. Grugeon, S. Laruelle, R. Herrera-Urbina, L. Dupont, P. Poizot, and J. M. Tarascon, *J. Electrochem. Soc.*, **148 (4)**, A285 (2001).
43) D. Larchera, G. Sudanta, J. B. Lerichea, Y. Chabreb, and J. M. Tarascon, *J. Electrochem. Soc.*, **149 (3)**, A234 (2002).
44) M. Dolle, P. Poizot, L. Dupont, and J. M Tarascon, Electrochem. *Solid-State Lett.*, **5 (1)**, A18 (2002).
45) S. Laruelle, S. Grugeon, P. Poizot, M. Dolle, L. Dupont, and J. M. Tarascon, *J. Electrochem. Soc.*, **149 (5)**, A627 (2002).
46) P. Poizot, S. Laruelle, S. Grugeon, and J. M. Tarascon, *J. Electrochem. Soc.*, **149 (9)**, A1212 (2002).
47) Z. Yuan, F. Huang, C. Feng, J. Sun, Y. Zhou, *Mater. Chem. Phys.*, **79 (1)**, 1 (2003).
48) P. Balaya, H. Li, L. Kienle, and J. Maier, *Adv. Funct. Mater.*, **13 (8)**, 621 (2003).
49) J. Hu, H. Li, and X. Huang, *Electrochem. and Solid-State Lett.*, **8 (1)**, A66 (2005).
50) W. Y. Li, L. N. Xu, and J. Chen, *Adv. Funct. Mater.*, **15**, 851 (2005).
51) F. Jiao, J. Bao, and P. G. Bruce, *Electrochem. and Solid-State Lett.*, **10 (12)**, A264 (2007).
52) J. Kim, M. K. Chung, B. H. Ka, J. H. Ku, S. Park, J. Ryu, and S. M. Oh, *J. Electrochem. Soc.*, **157 (4)**, A412 (2010).
53) D. Wadewitz, W. Gruner, M. Herklotz, M. Klose, L. Giebeler, A. Voß, J. Thomas, T. Gemming, J. Eckert, and H. Ehrenberg, *J. Electrochem. Soc.*, **160 (8)**, A1333 (2013).

54) R. Adam, D. Wadewitz, W. Gruner, V. Klemm, H. Ehrenberg, and D. Rafaja, *J. Electrochem. Soc.*, **160 (9)**, A1594 (2013).
55) Y. Zhou, W. Liu, M. Xue, L. Yu, C. Wu, X. Wu, and Z. Fu, *Electrochem. and Solid-State Lett.*, **9 (3)**, A147 (2006).
56) R. Prakash, C. Wall, A. K. Mishra, C. Kubel, M. Ghafari, H. Hahn, and M. Fichtner, *J. Power Sources*, **196**, 5936 (2011).
57) T. Nakajima, K. Dan, and M. Koh, *J. Fluorine Chem.*, **87**, 221 (1997).
58) R. Chandrasekaran, M. Koh, Y. Ozhawa, H. Aoyama, and T. Nakajima, *J. Chem. Sci.*, **121 (3)**, 339 (2009).
59) J. Yamaki, I. Yamazaki, M. Egashira, and S. Okada, *J. Power Sources.*, **102**, 288 (2001).
60) M. Ihara, B. T. Hang, K. Sato, M. Egashira, S. Okada, and J. Yamaki *J. Electrochem. Soc.*, **150 (11)**, A1476 (2003).
61) T. Tanaka, T. Doi, S. Okada, and J. Yamaki, F*uel Cells*, **9 (3)**, 269 (2009).
62) K. Sato, L. Zhao, S. Okada, and J. Yamaki, *J. Power Sources.*, **196**, 5617 (2011).
63) L. Zhao, S. Okada, and J. Yamaki, *J. Power Sources.*, **244**, 5617 (2013).
64) S. Dobashi, K. Nakanishi, H. Tanida, K. Hashizaki, Y. Uchimoto, T. Hirai, J. Yamaki, and Z. Ogumi, *J. Electrochem. Soc.*, **163 (5)**, A727 (2016).